Materials Science Forum
ISSN: 1662-9760, Vol. 879, pp 502-507
doi:10.4028/www.scientific.net/MSF.879.502

Evolution of Microstructure, Phase Composition and Hardness in 316L Stainless Steel Processed by High-Pressure Torsion

Moustafa El-Tahawy[1, *], Jenő Gubicza[1], Yi Huang[2], Hyelim Choi[3], Heeman Choe[3], János L. Lábár[4] and Terence G. Langdon[2]

[1] Department of Materials Physics, Eötvös Loránd University, Budapest, P.O.B. 32, H-1518, Hungary

[2] Materials Research Group, Faculty of Engineering and the Environment, University of Southampton, Southampton SO17 1BJ, UK

[3] School of Advanced Materials Engineering, Kookmin University, 77 Jeongneung-ro, Seongbuk-gu, Seoul 136-702, Republic of Korea

[4] Institute for Technical Physics and Materials Science, Centre for Energy Research, Hungarian Academy of Sciences, Budapest, Hungary

Keywords: High-Pressure Torsion, microstructure, hardness, stainless steel, austenite, martensite

Abstract. The evolution of phase composition, microstructure and hardness in 316L austenitic stainless steel processed by high-pressure torsion (HPT) was studied up to 20 turns. It was revealed that simultaneous grain refinement and phase transformation occur during HPT-processing. The γ-austenite in the initial material transformed gradually to ε- and α'-martensites due to deformation. After 20 turns of HPT the main phase was α'-martensite. The initial grain size of ~42 μm was refined to ~48 nm while the dislocation density increased to ~143 × 10^{14} m^{-2} in the α'-martensite phase at the disk periphery processed by 20 turns. The microstructure and hardness along the disk radius became more homogeneous with increasing numbers of turns. An approximately homogeneous hardness distribution with a saturation value of ~6140 MPa was achieved in 20 turns.

Introduction

The 316L austenitic stainless steel is frequently used as a structural material in biomedical and petrochemical applications as well as in nuclear power plants owing to its high strength, good ductility, high fracture toughness, excellent corrosion resistance and low neutron absorption [1-3]. The mechanical performance of 316L steel can be improved by severe plastic deformation (SPD) [4]. High-pressure torsion (HPT) is considered the most effective SPD technique in refinement of the grain structure down to the submicrometer or nanometer range [5-8]. The ultrafine-grained (UFG) or nanocrystalline microstructure produced during HPT-processing yields an improvement of the strength of materials.

It is well known that plastic deformation at low temperatures induces a phase transformation in austenitic steels from γ-austenite to ε and/or α'-martensites [9]. The path of martensite formation depends on the stacking fault energy (SFE) and therefore on the chemical composition [10]. The following sequences of martensitic transformation have been observed: γ→ε, γ→ε→α' and γ→α' [9-11]. The development of ε-martensite phase with hexagonal close-packed (hcp) structure from face-centered cubic (fcc) γ-austenite is related to the low SFE of stainless steels. If stacking faults are formed on every second {111} plane of the fcc lattice, the fcc sequence ABCABC transforms into hcp sequence ABABAB. Therefore, gliding of Shockley partial dislocations during deformation may yield the appearance of ε-martensite phase. Then, the bands of ε-phase can serve as nucleation sites for the α'-phase [11-12]. The aim of this work is to study the evolution of phase composition, microstructure and hardness in 316L austenitic stainless steel processed by HPT at room temperature.

Material and experimental procedures

The investigated material was a 316L type austenitic stainless steel with the composition of Fe - 17.20% Cr - 8.97% Ni - 2.13% Mo - 1.03% Mn - 0.77% Si - 0.48% Cu - 0.35% Co (in wt. %) as determined by energy dispersive X-ray spectroscopy. Initially, in order to obtain a single phase γ-austenite with coarse-grained microstructure, the material was annealed at 1100°C for 1 h, then quenched to room temperature. Disks with diameter of 9.85 mm and thickness of ~0.85 mm were processed by HPT operating under quasi-constrained conditions with an applied pressure of 6.0 GPa and a rate of 1 rpm at room temperature [13]. The HPT deformation was carried out for ¼, ½, 1, 3, 5, 10 and 20 revolutions.

The cross sectional microstructures of the initial and the HPT-processed disks were examined with an FEI Quanta 3D scanning electron microscope (SEM). The electron backscatter diffraction (EBSD) images were taken with a step size of 30 nm. The nanocrystalline microstructure at the disk periphery was examined using a Philips CM20 transmission electron microscope (TEM) operating at 200 keV. The phase composition and the microstructural parameters were investigated by X-ray diffraction (XRD). The XRD diffractograms were measured on the disk surface using a high-resolution diffractometer with $CoK_{\alpha 1}$ radiation (wavelength: $\lambda = 0.1789$ nm). The X-ray line profile analysis (XLPA) was carried out with the Convolutional Multiple Whole Profile (CMWP) fitting method in order to determine the crystallite size and the dislocation density in the HPT-processed disks [14]. The following microstructural parameters were obtained from the CMWP fitting method: the area-weighted mean crystallite size ($\langle x \rangle_{area}$) and the mean dislocation density (ρ). The value of $\langle x \rangle_{area}$ was calculated as $\langle x \rangle_{area} = m \exp(2.5\sigma^2)$, where m is the median and σ^2 is the log-normal variance of the crystallite size distribution. The Vickers microhardness was measured on the disk surface along the diameters of the initial and the HPT-processed disks using a Zwick Roell ZHμ hardness tester with an applied load of 0.5 kg and a dwell time of 10 s.

Results and discussion

Phase transformation during HPT. Fig. 1a and b illustrate the change of phase composition in the center and the periphery of the HPT-processed disks, respectively. The initial sample is mainly γ-austenite with a very small fraction of α'-martensite (~3%). The XRD diffractograms show that phase transformation was induced by HPT from γ-austenite into ε- and α'-martensites. The martensite transformation was observed even in the early stage of deformation at the center of the disk processed by HPT for ¼ turn. With increasing the number of turns and distance from the disk center, the transformation is more pronounced. At the periphery of the disk processed by 20 turns, where the strain is the highest, the material is almost a single phase α'-martensite.

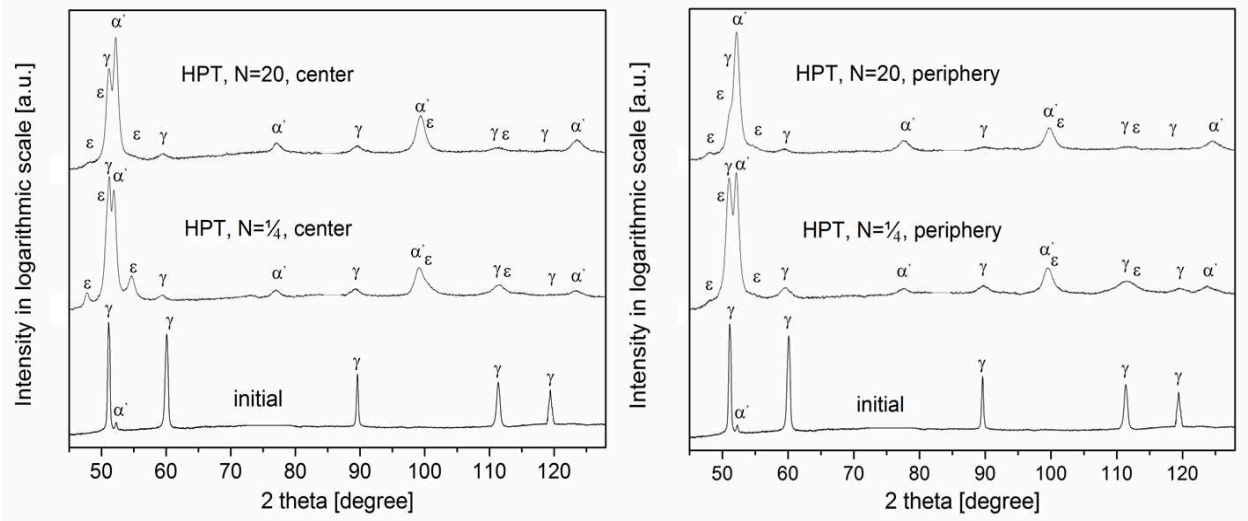

Fig. 1. X-ray diffraction patterns obtained for (a) the center and (b) the periphery of the initial material and HPT-processed disks for N=¼ and 20 turns. Note that the intensity is in logarithmic scale.

The XRD and EBSD experiments revealed that the amounts of ε and α'-martensites strongly depend on the strain induced by HPT. The fraction of ε-phase first increased with increasing HPT revolutions; however at high number of turns it decreased and α'-martensite became the dominant phase. According to this observation, the transformation sequence γ→ε→α' is suggested for 316L steel processed by HPT. EBSD investigations (not shown here) showed that α'-martensite grains were nucleated inside ε-martensite bands, i.e. the ε-phase acts as an intermediary phase in the formation of α'-martensite from γ-austenite.

Microstructure evolution during HPT-processing. Typical cross-sectional microstructures in the initial material and the disks processed by HPT for different numbers of revolutions from ¼ to 20 are shown in Fig. 2. The initial material has a uniform coarse-grained microstructure with a mean grain size of ~42 μm. A highly non-uniform microstructure was observed along the radius of HPT-processed disks for low numbers of revolutions. At the center of the disk processed for N=¼ there is a slight grain refinement to ~25 μm, while far from the center a fine-grained flow pattern with bright and dark strips was formed (see Fig. 2). Energy-dispersive X-ray spectroscopy in SEM revealed no significant difference between the chemical compositions of these two regions. Additional EBSD investigations (not shown here) indicated that the contrast for ε-martensite in the SEM images is brighter than for γ-austenite or α'-martensite. Therefore, the brighter contrast in the flow pattern corresponds to a larger fraction of ε-martensite. As the number of revolutions increased, the UFG flow pattern spread towards the disk center. A homogeneous cross-sectional microstructure was achieved after 20 turns of HPT. Moreover, cracks were developed for numbers of turns larger than three.

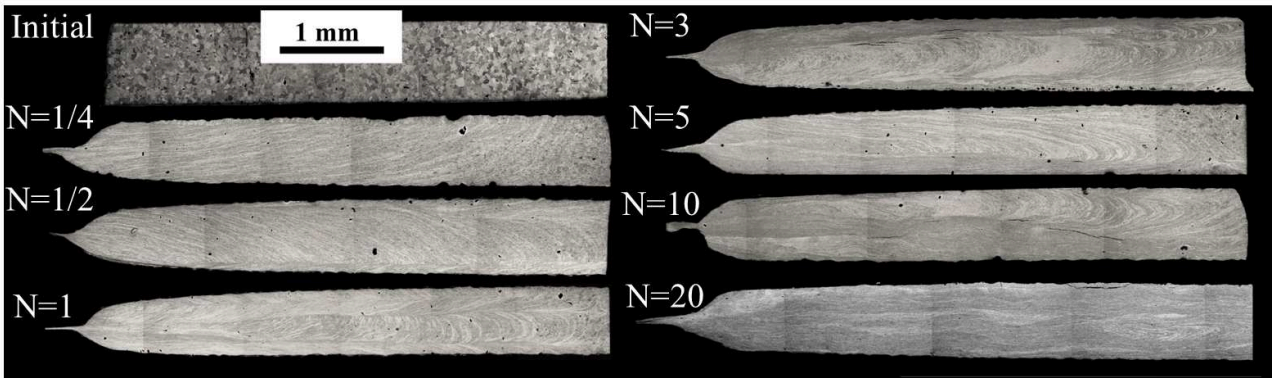

Fig. 2. The cross-sectional microstructure in the initial material and in the disks processed by HPT for different numbers of turns from ¼ to 20.

Fig. 3 shows EBSD images taken on the cross-section of the initial sample and at the center of the HPT disk processed for ½ turn. The initial material exhibits a coarse-grained γ-austenite with a mean grain size of ~42 μm. The microstructure after HPT-processing for ½ turn contains three phases: γ-austenite, ε-martensite and α'-martensite, as shown in Figs. 3b, c and d, respectively. The morphology of the γ-austenite and ε-martensite phases reflects the role of stacking faults in the transformation from γ- to ε-phase. In this sample, if the distance from the disk center is larger than one-eighth of the radius, EBSD is unable to resolve the very fine grains, therefore an additional TEM study was performed.

Table 1 lists the grain size values obtained by TEM at the disk periphery for different numbers of turns. The mean grain size decreased from ~42 μm in the initial material to ~120 nm at the disk periphery even after ¼ turn of HPT. A further reduction in grain size was observed with increasing numbers of HPT revolutions and after 20 turns the mean grain size was refined to ~48 nm.

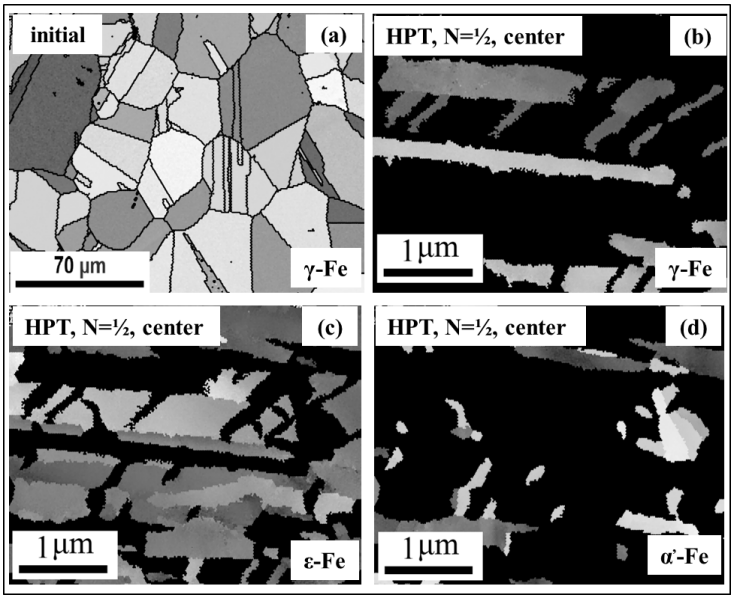

Fig. 3. EBSD images for (a) the initial sample and the center of the HPT disk processed for ½ turn: (b) γ-austenite (c) ε-martensite and (d) α'-martensite.

The samples processed by HPT have broad peaks in the X-ray diffraction patterns (see Fig. 1). The evaluation of the line profiles provides the values of the microstructural parameters in the HPT-processed 316L steel. Due to the strongly overlapping peaks of γ-austenite and ε-martensite (see Fig. 1), the line profiles of these phases were not evaluated. Therefore, the parameters of the microstructure were determined only for α'-martensite. A major attempt was undertaken to determine the crystallite size and the dislocation density characterizing relatively large volumes in the samples, and thus the XRD patterns were evaluated only in the peripheral regions of the disks where α'-martensite was the major phase. The crystallite size and the dislocation density values are listed in Table 1. It was found that the crystallite size decreased from ~37 to ~24 nm while the dislocation density increased from ~66 × 10^{14} m^{-2} to ~143 × 10^{14} m^{-2} with increasing numbers of HPT turns from ¼ to 20. It is worth noting that the crystallite size is very small and the dislocation density is very high at the disk periphery already after ¼ turn. It is noted that the crystallite size for all samples is smaller than the grain size obtained by TEM by a factor of ~2-4. This difference can be explained by the fact that XLPA measures the size of the sub-grains or dislocation cells rather than the true grain size.

Table 1. The grains size estimated by TEM, the mean crystallite size and the dislocation density determined by XLPA and the hardness measured by Vickers indenter, at peripheral regions of the disks processed by HPT for different numbers of turns.

Number of turns	Grain size [nm]	Crystallite size [nm]	Dislocation density [10^{-14} m^{-2}]	Hardness [MPa]
¼	120	37 ± 4	66 ± 7	4905 ± 150
½	105	27 ± 1	73 ± 8	5145 ± 156
1	70	26 ± 3	86 ± 9	5200 ± 160
3	60	26 ± 4	88 ± 9	5317 ± 167
5	53	25 ± 2	101 ± 10	5758 ± 182
10	45	22 ± 2	133 ± 12	6126 ± 189
20	48	24 ± 3	143 ± 13	6140 ± 195

Hardness evolution along the disk radius. Figure 4 shows the hardness distributions along the diameter of the initial and some selected HPT-processed disks. The hardness of HPT disks gradually increases from the center towards the periphery and also with increasing numbers of HPT revolutions. This observation is in accordance with the increase of the strain for larger distance from the center and higher numbers of turns. The early stage of HPT deformation is accompanied by significant hardening, as the hardness rapidly increased from ~1410 MPa in the initial state to ~3816

and ~4905 MPa in the center and the periphery of the disk processed for ¼ turn, respectively. At the periphery of the disks, saturation of the hardness with a value of ~6126 MPa was achieved after 10 turns of HPT. A further increment in the number of passes yielded no significant improvement in the hardness at the disk periphery. At the same time, in the disk center considerable hardening was observed between 10 and 20 revolutions of HPT. An almost homogeneous hardness distribution along the disk radius was achieved only after 20 turns.

The large increment in the hardness already after ¼ turn is in accordance with the strong refinement of the microstructure at low strains. In the disk center the large initial γ-austenite grains were fragmented into much smaller regions due to the nucleation of grains of ε- and α'-martensites. In addition, the dislocation density increased to large values at the periphery (see Table 1) which also contributed to grain refinement since a fraction of dislocations was most probably arranged into subgrain/grain boundaries. In the periphery, where the strain is the highest along the disk radius, the grain size was reduced to ~120 nm even after ¼ turn. Then, there is a gradual increment in the dislocation density and a reduction in the grain size at the disk periphery. However, after 10 turns a significant change in the microstructure was not observed in accordance with the hardness evolution. In the center, the hardness saturation was achieved at higher numbers of turns due to the slower increase of strain as a function of HPT revolutions.

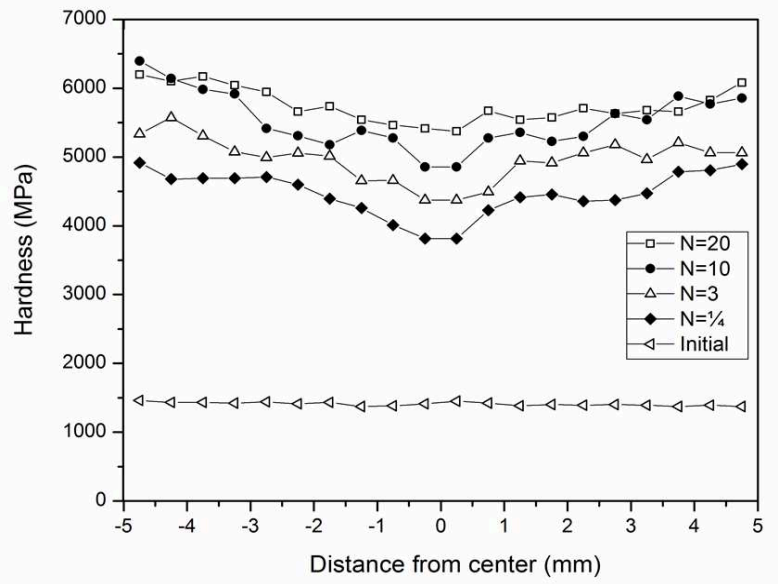

Fig. 4. The radial distribution of microhardness values for different numbers of HPT turns.

Conclusions

The phase composition, the microstructure and the hardness evolutions in coarse-grained 316L austenitic stainless steel processed by HPT were investigated. The following conclusions have been drawn:

1. The HPT-induced phase change from γ-austenite into ε- and α'-martensites with the transformation sequence γ→ε→α' was observed. First, ε-martensite bands were formed inside the coarse γ-austenite grains, then α'-martensite grains were nucleated in the ε-martensite phase. Accordingly, first the amount of ε-martensite increased, however for higher number of turns its fraction decreased. At the same time, the amount of α'-martensite increased monotonously with increasing numbers of revolutions and after 20 turns this is the main phase at the disk periphery.
2. HPT yielded a strong reduction in the mean grain size from ~42 μm in the initial material to ~48 nm at the disk periphery after 20 turns of HPT. Extremely small crystallite size (subgrain size) and high dislocation density in the main α'-martensite phase with values of ~24 nm and ~143 × 10^{14} m^{-2}, respectively, were detected at the periphery of the disk processed for 20 turns.
3. Both the microstructure and the hardness show a high degree of heterogeneity along the disk radius for low numbers of turns. At the disk center coarse grains were observed, although their

interiors were fragmented due to the phase transformation. The multiphase microstructure yielded a strong hardening in the disk center even after ¼ turn of HPT. At the disk periphery the very high dislocation density and the associated grain refinement caused additional hardening. The degree of homogeneity increased with increasing numbers of turns and after 20 revolutions the hardness in the center was only slightly lower than at the periphery. A very high saturation value of the hardness (~6140 MPa) was measured at the periphery of the disk processed by 20 turns which can be attributed to the very high dislocation density and grain size values.

Acknowledgements

This study was supported by the Hungarian Scientific Research Fund, OTKA, Grant No. K-109021. The authors are grateful to Mr. Gabor Varga for the SEM and EBSD investigations. The first author was supported by the executive program between the Egyptian and the Hungarian Governments. YH and TGL were supported by the European Research Council under ERC Grant Agreement No. 267464-SPDMETALS.

References

[1] G.L. Lucas, F.W. Cooke, E.A. Friis, A primer of biomechanics, Springer Science + Business Media, New York, NY, 1999.
[2] I. Gotman, Characteristics of metals used in implants, Endourology, 11 (1997) 383-389.
[3] Y. Kim, Y. Kim, D. Kim, S. Kim, W. Nam, H. Choe, Effects of hydrogen diffusion on the mechanical properties materials of austenite 316L steel at ambient temperature, Materials Transactions, 52 (2011) 507-513.
[4] S. Scheriau, Z. Zhang, S. Kleber, R. Pippan, Deformation mechanisms of a modified 316L austenitic steel subjected to high pressure torsion, Materials Science and Engineering: A, 528 (2011) 2776-2786.
[5] A.P. Zhilyaev, T.G. Langdon, Using high-pressure torsion for metal processing: Fundamentals and applications, Progress in Materials Science, 53 (2008) 893-979.
[6] T.G. Langdon, Twenty-five years of ultrafine-grained materials: Achieving exceptional properties through grain refinement, Acta Materialia, 61 (2013) 7035-7059.
[7] R.Z. Valiev, A.P. Zhilyaev, T.G. Langdon, Bulk Nanostructured Materials: Fundamentals and Applications, John Wiley & Sons, Inc., Hoboken, New Jersey, 2014.
[8] R.Z. Valiev, R.K. Islamgaliev, I.V. Alexandrov, Bulk nanostructured materials from severe plastic deformation, Progress in Materials Science, 45 (2000) 103-189.
[9] V. Seetharaman, R. Krishnan, Influence of the martensitic transformation on the deformation behaviour of an AISI 316 stainless steel at low temperatures, Materials Science and Engineering: A, 16 (1981) 523-530.
[10] R.E. Schramm, R.P. Reed, Stacking fault energies of seven commercial austenitic stainless steels, Metallurgical Transactions A, 6 (1975) 1345-1351.
[11] J.A. Venables, The martensite transformation in stainless steel, Philosophical Magazine, 7 (1962) 35-44.
[12] R. Lagneborgj, The martensite trnsformation in 18% Cr-8% Ni steels, Acta Metallurgica, 12 (1964) 823-843.
[13] R.B. Figueiredo, P.H.R. Pereira, M.T.P. Aguilar, P.R. Cetlin, T.G. Langdon, Using finite element modeling to examine the flow processes in quasi-constrained high-pressure torsion, Acta Materialia, 60 (2012) 3190-3198.
[14] G. Ribárik, J. Gubicza, T. Ungár, Correlation between strength and microstructure of ball-milled Al–Mg alloys determined by X-ray diffraction, Materials Science and Engineering: A, 387-389 (2004) 343-347.